Investigating electron interacting dark matter

R. Bernabei, P. Belli, F. Montecchia, and F. Nozzoli
Dipartimento di Fisica, Università di Roma "Tor Vergata" and INFN, Sezione Roma "Tor Vergata", I-00133 Rome, Italy

F. Cappella, A. Incicchitti, and D. Prosperi
Dipartimento di Fisica, Università di Roma "La Sapienza" and INFN, Sezione Roma, I-00185 Rome, Italy

R. Cerulli
Laboratori Nazionali del Gran Sasso, INFN, Assergi, Italy

C. J. Dai, H. L. He, H. H. Kuang, J. M. Ma, X. H. Ma, X. D. Sheng, Z. P. Ye,* R. G. Wang, and Y. J. Zhang
IHEP, Chinese Academy, P.O. Box 918/3, Beijing 100039, China
(Received 20 November 2007; published 10 January 2008)

Some extensions of the standard model provide dark matter candidate particles which can have a dominant coupling with the lepton sector of the ordinary matter. Thus, such dark matter candidate particles (χ^0) can be directly detected only through their interaction with electrons in the detectors of a suitable experiment, while they are lost by experiments based on the rejection of the electromagnetic component of the experimental counting rate. These candidates can also offer a possible source of the 511 keV photons observed from the galactic bulge. In this paper this scenario is investigated. Some theoretical arguments are developed and related phenomenological aspects are discussed. Allowed intervals and regions for the characteristic phenomenological parameters of the considered model and of the possible mediator of the interaction are also derived considering the DAMA/NaI data.

DOI: 10.1103/PhysRevD.77.023506 PACS numbers: 95.35.+d

I. INTRODUCTION

Dark matter particles with dominant interaction on electrons have been considered in literature [1–4]. In particular, from a phenomenological point of view, dark matter (DM) candidates with electron interactions can offer possible sources for the 511 keV positron annihilation line observed from the galactic bulge [5,6]. These candidates can be either light (MeV scale) [1] or heavy (GeV or larger scale) [2,3]. They are expected to interact with electrons both through neutral light (MeV scale) U or Z' bosons or through heavy charged mediators $\chi^\pm$ (which can eventually be nearly degenerate with χ^0) [3]. Recently data collected by some accelerator experiments have been analyzed in terms of a $\sim$200 MeV neutral boson which couples to quarks with flavor changing transition: $s \rightarrow d\mu^+\mu^-$ [7,8]. Other results showing some resonances at energies lower than the two-muon [7] and the two-pion [9] disintegration thresholds have been associated with a Goldstone neutral boson of $\sim$20 MeV mass. Moreover, some excess has been achieved in dedicated experiments on low energy nuclear reactions searching for possible $e^+ - e^-$ pairs driven by the presence of a neutral boson with a mass around 10 MeV [10].

Let us remark that—in the frameworks where the mediator is either a ±1 charged boson or a neutral boson providing a flavor changing transition among quarks—the elastic scatterings of the DM candidate χ^0 particles on nuclei would be either forbidden or suppressed; hence, the scattering on electrons would remain the unique possibility for the direct detection of the χ^0 particles.

On the other hand, from a pure theoretical point of view, it is also conceivable that the mediator of the DM particle interactions can be coupled only to the lepton sector of the ordinary matter. Thus, in this case the DM particles can just interact with electrons and cannot with nuclei. This is suggested in Ref. [4] for the U boson and can also be the case of some extensions[1] of the standard model providing a quark-lepton discrete symmetry $SU(3)_l \times SU(3)_q \times SU(2)_L \times U(1)$. In these latter models, leptons (as well as quarks) are assumed to have three "leptonic (l) colors" and to interact through the gauge group $SU(3)_l$, analogously as the QCD color group $SU(3)_q$. Moreover, at some high energy scale a symmetry breaking $SU(3)_l \rightarrow SU(2)'$ is expected, giving high mass to the "exotic" leptonic degree of freedom and leaving light the "standard" leptons [13]. In these scenarios, the heavy exotic leptonic degree of freedom provides both heavy charged $\pm1/2$ fermions, which are expected to be confined into exotic *leptonic hadrons* by the unbroken gauge group $SU(2)'$ [13], and heavy neutrinos [12,13]; hence, they can be considered as dark matter candidates with dominant interaction on electrons.

*Also at University of Jing Gangshan, Jiangxi, China.

[1]Some examples are the models from the extended Pati-Salam gauge group $SU(6) \times SU(2)_L \times SU(2)_R$ [11] or those from $[SU(3)]^4$ quartification [12].

Moreover, it is worth noting that other possibilities can exist. For example, supersymmetric (SUSY) theories can offer configurations in the general SUSY parameter space where the lightest supersymmetric particle (LSP) has an interaction with an electron dominant with respect to that with quark.

These DM candidate particles can be directly detected only through their interaction with electrons in the detectors of a suitable experiment, while they are lost by experiments based on the rejection of the electromagnetic component of the experimental counting rate.

In the present paper this kind of DM candidates is investigated, some theoretical arguments are developed, and related phenomenological aspects are discussed. In particular, the impact of these DM candidates will also be discussed in a phenomenological framework on the basis of the 6.3σ C.L. DAMA/NaI model independent evidence for particle dark matter in the galactic halo [14,15]. We remind that various corollary analyses, considering some of the many possible astrophysical, nuclear, and particle physics scenarios, have been analyzed by DAMA itself both for some WIMP/WIMP-like candidates and for light bosons [14–19], while several others are also available in literature, such as e.g. Refs. [20–30]. Many other scenarios can be considered as well. At present, the new second generation DAMA/LIBRA setup is running at the Gran Sasso Laboratory.

II. DETECTABLE ENERGY IN χ^0—ELECTRON ELASTIC SCATTERING

The practical possibility to detect electron interacting DM candidates (hereafter χ^0 with mass m_{χ^0} and 4-momentum k_μ) is based on the detectability of the energy released in χ^0-electron elastic scattering processes (see Fig. 1).

Generally, these processes are not taken into account in the DM field since the electron is assumed at rest and, therefore, considering the χ^0 particle velocity $|\vec{v}_{\chi^0}| \sim 300$ km/s, the released energy is of the order of few eV, well below the detectable energy in any considered detector in the field. However, the electron is bound in the atom and, even if the atom is at rest, the electron can have not negligible momentum, p. For example, the bound electrons in NaI(Tl) offer a probability equal to $\sim 1.5 \times 10^{-4}$ to have $p \gtrsim 0.5$ MeV$/c$; such a probability is quite small, but not zero. Hence, interactions of χ^0 particles with these high-momentum electrons in an atom at rest can give rise to detectable signals in suitable detectors. In particular, after the interaction the final state can have—beyond the scattered χ^0 particle—either a prompt electron and an ionized atom or an excited atom plus possible x-rays/Auger electrons. Therefore, the process produces x rays and electrons of relatively low energy, which are mostly contained with efficiency ~ 1 in a detector of a suitable size. Thus, the total detected energy, $E_d = k_0 - k_0' = p_0' - p_0$ (where k_0, k_0', p_0', and p_0 are the time components of the respective 4-vectors in the laboratory frame, see Fig. 1), can be evaluated considering the energy conservation in the center of mass (CM) frame of the $\chi^0 - e^-$ system. Defining $\vec{\beta} = \frac{\vec{k}+\vec{p}}{k_0+p_0}$ as the velocity of the CM frame with the respect to the laboratory frame and $\gamma = 1/\sqrt{1-\beta^2}$ Lorentz boost factor, one can write the energies of the electron before and after the scattering by using the variables in the CM frame through the Lorentz transformations:

$$p_0 = \gamma(p_{0,\mathrm{CM}} + \vec{\beta}\cdot\vec{p}_{\mathrm{CM}}) \quad \text{and} \quad p_0' = \gamma(p_{0,\mathrm{CM}}' + \vec{\beta}\cdot\vec{p'}_{\mathrm{CM}}). \tag{1}$$

Since we are dealing with elastic scattering, $p_{0,\mathrm{CM}} = p_{0,\mathrm{CM}}'$ and $|\vec{p}_{\mathrm{CM}}| = |\vec{p}_{\mathrm{CM}}'|$, so that, by subtraction, one obtains

$$E_d = \gamma(\vec{\beta}\cdot\vec{p}_{\mathrm{CM}}' - \vec{\beta}\cdot\vec{p}_{\mathrm{CM}}) = \gamma\beta p_{\mathrm{CM}}(\cos\theta' - \cos\theta), \tag{2}$$

where θ' is the angle between $\vec{\beta}$ and $\vec{p}_{\mathrm{CM}}'$, θ is the angle between $\vec{\beta}$ and $\vec{p}_{\mathrm{CM}}$, and $\vec{p}_{\mathrm{CM}} = \gamma(\vec{p} - \vec{\beta}p_0)$.

Therefore, fixing the input momenta of the χ^0 particle ($\vec{k}$) and of the electron ($\vec{p}$), the maximum detected energy is given by $E_+ = \gamma\beta p_{\mathrm{CM}}(1-\cos\theta)$. Few examples of the dependence of E_+ on the χ^0 mass are given in Fig. 2 as a function of the electron's momentum and of the χ^0 velocities for head-on collisions ($\theta = \pi$). Figure 2 also points out that χ^0 particles with m_{χ^0} larger than few GeV can provide sufficient energy to be detected in a suitable detector.

It is interesting to explore two limit cases (remind that owing to the typical χ^0 velocities, $k_0 \simeq m_{\chi^0}$ and $\vec{k} \simeq m_{\chi^0}\cdot\vec{v}_{\chi^0}$; hereafter $c = 1$):

(a) $p \ll \beta m_e \sim$ keV, that is target nearly at rest:[2] $E_+ \simeq 2\beta^2 m_e \sim$ eV.

(b) $k \gg p \gg \beta p_0 \sim$ keV; in this case one obtains $\vec{p}_{\mathrm{CM}} \simeq \vec{p}$, $\vec{\beta} \simeq \vec{v}_{\chi^0}$, and, therefore, θ is also the angle

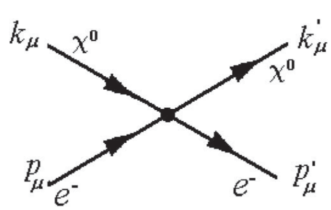

FIG. 1. The $\chi^0 - e^-$ elastic scattering and definition of the momentum variables in the laboratory frame. In the text a contact interaction has been assumed (also see Appendix B) as a suitable approximation of the process.

[2]We note that in general for a target of mass m_T nearly at rest, $E_+ \simeq 2\beta^2 m_T = \frac{1}{2}m_{\chi^0}v_{\chi^0}^2\frac{4m_{\chi^0}m_T}{(m_{\chi^0}+m_T)^2}$; that is, one gets the formula describing, for example, the WIMP-nucleus elastic scattering.

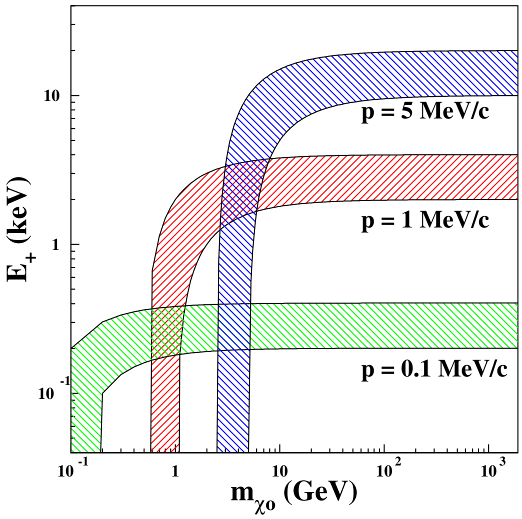

FIG. 2 (color online). A few examples of the dependence of the maximum released energy, E_+, on the χ^0 mass for the electron's momenta of 0.1, 1, and 5 MeV$/c$, for v_{χ^0} ranging in the interval 1–2 $\times 10^{-3}c$ and for head-on collisions ($\theta = \pi$).

between $\vec{p}$ and $\vec{k}$. Hence, $E_+ \simeq v_{\chi^0} p(1 - \cos\theta)$. This is the case of interest for the direct detection; in fact, for m_{χ^0} larger than few GeV k is larger than the maximum momentum of a bound electron in the atom due to the finite size of the nucleus ($\sim$ 15 MeV in iodine).

In conclusion, χ^0 particles with mass $\gtrsim$ few GeV, interacting on bound electrons with momentum up to $\simeq$ few MeV$/c$ [see case (b)], can provide signals in the keV energy region detectable by low background and low energy threshold detectors, such as those of DAMA/NaI (see later).

III. CROSS SECTION AND COUNTING RATE

A. The cross section at fixed electron momentum

The differential cross section for χ^0-electron elastic scattering can be written as

$$d\sigma = \frac{\overline{|M|^2}}{v_{(\chi^0 e)}} \frac{1}{2k_0 2p_0} (2\pi)^4 \delta^4(k + p - k' - p') \times \frac{d^3p'}{(2\pi)^3 2p'_0} \frac{d^3k'}{(2\pi)^3 2k'_0}. \tag{3}$$

There $\overline{|M|^2}$ is the averaged squared matrix element and $v_{(\chi^0 e)}$ is the relative velocity between χ^0 and the electron.

Integrating over d^3k' and over the p' solid angle and considering that $p'dp' = p'_0 dp'_0 = p'_0 dE_d$, one can write

$$\frac{d\sigma}{dE_d} = \frac{\overline{|M|^2}}{32\pi v_{(\chi^0 e)} k_0 p_0} \frac{1}{|\vec{k} + \vec{p}|} \Theta(E_+ - E_d). \tag{4}$$

The Heaviside theta function defines the domain of the differential cross section.

It is useful in the following to define the χ^0 cross section on the electron at rest ($p = 0$); thus, one can write

$$\left.\frac{d\sigma}{dE_d}\right|_{(p=0)} = \frac{\overline{|M|^2}_{(p=0)}}{32\pi v_{\chi^0} k_0 m_e} \frac{1}{k} \Theta(E_+ - E_d) = \frac{\sigma_e^0}{E_+} \Theta(E_+ - E_d), \tag{5}$$

where $E_+(p = 0) = 2m_e v_{\chi^0}^2 \sim$ eV and $\sigma_e^0 = \frac{\overline{|M|^2}_{(p=0)}}{16\pi m_{\chi^0}^2}$. In the following, for simplicity, we define $\sigma_e = \frac{\overline{|M|^2}}{16\pi m_{\chi^0}^2}$, then $\sigma_e(p = 0) = \sigma_e^0$.

B. The cross section for atomic electrons

Let us now introduce in the previous evaluations the momentum distribution of the electrons in the atom, $\rho(\vec{p})$ (see Appendix A). In particular, from Eq. (4)—that is for a fixed $\vec{p}$ value—one can write for the atomic case

$$\frac{d\sigma}{dE_d} = \frac{\overline{|M|^2}}{32\pi v_{(\chi^0 e)} k_0 p_0} \frac{1}{|\vec{k} + \vec{p}|} \Theta(E_+ - E_d) \rho(\vec{p}) d^3p. \tag{6}$$

Introducing the σ_e definition and replacing E_+ with its expression, it is possible to write for the relevant case of direct detection ($k \gg p \gg m_e v_{\chi^0}$)

$$\frac{d\sigma}{dE_d} \simeq \frac{\sigma_e p^2}{2 v_{(\chi^0 e)} v_{\chi^0} p_0} \rho(\vec{p}) d\phi d\cos\theta \times \Theta[v_{\chi^0} p(1 - \cos\theta) - E_d] dp; \tag{7}$$

here the polar axis has been chosen in the direction of $\vec{k}$.

The integration over ϕ simply gives 2π considering that $\overline{|M|^2}$ does not depend on ϕ and that atoms with full shells (as Na^+ and I^-) have isotropic distributions $\rho(p)$.

C. The counting rate

The expected interaction rate of the χ^0 particle impinging on the electrons of an atom can be derived as

$$\frac{dR}{dE_d} = \frac{\rho_{\chi^0}}{m_{\chi^0}} \eta_e \int \frac{d\sigma}{dE_d} v_{(\chi^0 e)} f(\vec{v}_{\chi^0}) d^3 v_{\chi^0}, \tag{8}$$

where (i) $\rho_{\chi^0} = \xi \rho_0$ with ρ_0 local halo density and $\xi \leq 1$ fractional amount of χ^0 density in the halo; (ii) $f(\vec{v}_{\chi^0})$ is the χ^0 velocity (v_{χ^0}) distribution in the Earth frame; (iii) η_e is the electron's number density in the target material.

In the reasonable hypothesis that σ_e does not depend on $\cos\theta$, the integrand in Eq. (8) can be evaluated considering that

$$\frac{d\sigma}{dE_d}v_{(\chi^0 e)} = \frac{2\pi\sigma_e p^2}{v_{\chi^0}^2 p_0}\rho(p)(v_{\chi^0} - v_{\min})\Theta(v_{\chi^0} - v_{\min})dp, \tag{9}$$

where $v_{\min} = \frac{E_d}{2p}$ is the minimal χ^0 particle velocity in order to provide an energy E_d released in the detector.

The matrix element $|M|^2$—as well as σ_e in Eq. (9)—can generally depend on p and v_{χ^0}. Thus, in order to evaluate it, it is necessary to consider a specific particle interaction model (see Appendix B).

For simplicity, we will consider a 4-fermion contact interaction (e.g. a mediator with mass larger than many MeV, neglecting the 4-momentum transferred into the propagator). Thus, for the cases of pure $V \pm A$ and pure scalar interactions—which are addressed in the following—one gets $\sigma_e \simeq \sigma_e^0 \frac{p_0^2}{m_e^2}$. Other interaction models are possible and can be investigated in the future. It is worthwhile to stress that—although the calculations are made for the $V \pm A$ and for the scalar 4-fermion contact interactions—the same results can be achieved for any kind of DM candidate interacting with electrons and with cross section σ_e having a weak dependence on p and v_{χ^0}, that is $\sigma_e \sim \sigma_e^0$.

Finally, the expected interaction rate can be written as

$$\frac{dR}{dE_d} = \frac{\xi\sigma_e^0}{m_{\chi^0}}\frac{2\pi\rho_0}{m_e^2}\eta_e\int_0^\infty p^2 p_0 \rho(p) I(v_{\min})dp, \tag{10}$$

where—pointing out the time dependence of $f(\vec{v}_{\chi^0})$—we have introduced the useful function,

$$\begin{aligned} I(v_{\min}) &= \int_{v_{\min}}^\infty \frac{f(\vec{v}_{\chi^0})}{v_{\chi^0}^2}(v_{\chi^0} - v_{\min})d^3 v_{\chi^0} \\ &\simeq I_0(v_{\min}) + I_m(v_{\min})\cos\omega(t - t_0). \end{aligned} \tag{11}$$

Here roughly $t_0 \simeq$ 2nd June and $\omega = \frac{2\pi}{T}$ with $T = 1$ yr. The cutoff of the halo escaping velocity is included into the $f(\vec{v}_{\chi^0})$ function distribution.

Therefore, the expected counting rate accounting for the energy resolution of the detector can be written as

$$\frac{dR}{dE} = \int G(E, E_d)\frac{dR}{dE_d}dE_d = S_0 + S_m\cos\omega(t - t_0), \tag{12}$$

where S_0 and S_m are the unmodulated and the modulated part of the expected signal, respectively. The $G(E, E_d)$ kernel generally has a Gaussian behavior.

Finally, we note that—since m_{χ^0} is larger than few GeV (so that $k \gg p$)—the expected counting rate has a simple dependence upon σ_e^0 and m_{χ^0}; therefore, the ratio $\frac{\xi\sigma_e^0}{m_{\chi^0}}$ is a normalization factor of the expected energy distribution.

The momentum distribution of the electrons in NaI(Tl), $\rho(p)$, has been depicted in Fig. 3(a); it has been calculated from the corresponding Compton profile, $J(p)$, reported in Ref. [31]. For this purpose, due to the isotropic distributions of Na^+ and I^- (ions with full shells), the relation $J(p) = 2\pi\int_p^\infty \rho(q)qdq$ has been used [32,33]. At high momentum the $\rho(p)$ function follows the hydrogenic behavior of the $1s$ internal shell of the iodine atom: $\rho(p) \propto (p_I^2 + p^2)^{-4}$ with $p_I \simeq 200$ keV.

As an example, in Fig. 3(a) the behaviors of $I_0(v_{\min})$, $I_m(v_{\min})$, and $\rho(p)$ are compared as a function of the electron's momentum, p, for NaI(Tl) as target material and for the given released energy: $E_d = 3$ keV. In this figure as a template the considered halo model is the A5 model of Refs. [14,34], that is a Navarro, Frenk, and White (NFW) halo model with local velocity equal to 220 km/s and density equal to the maximum value ($\rho_0 =$ 0.74 GeV cm^{-3}).

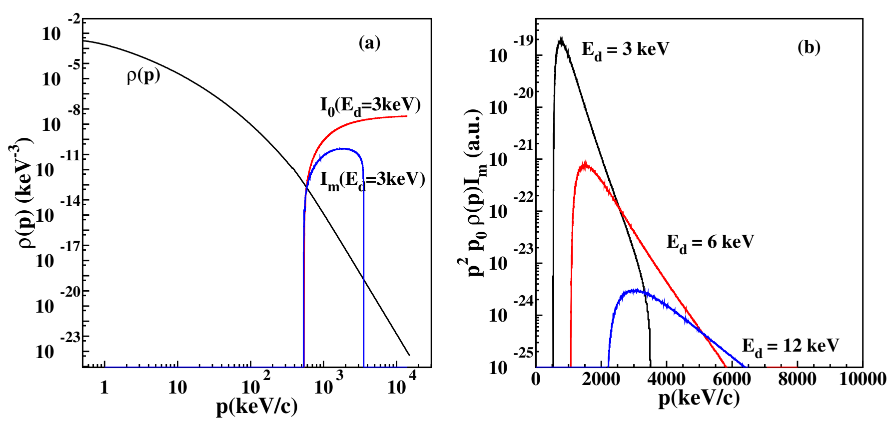

FIG. 3 (color online). (a) Behaviors of $\rho(p)$ (solid black line) for NaI(Tl) and I_0 and I_m for $E_d = 3$ keV in the considered halo model, A5 of Ref. [14,34]; see also text. The functions I_0 and I_m are in arbitrary units. (b) Behaviors of $p^2 p_0 \rho(p) I_m$ for NaI(Tl) at three different values of the released energy: $E_d = 3$, 6, and 12 keV in the considered halo model, A5 of Ref. [14,34]; they show as the main contribution to the counting rate in NaI(Tl) detectors with energy threshold at 2 keV comes from electrons with momenta around few MeV/c.

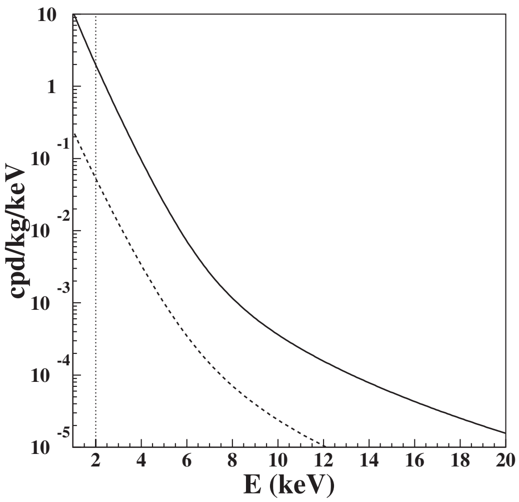

FIG. 4. An example of the shapes of expected energy distributions in NaI(Tl) due to χ^0 interactions with electrons for the scenario given in the text; the solid line gives the behavior of the unmodulated part of the expected signal, S_0, while the dashed line is the behavior of the modulated part, S_m. In this example the normalization factor is $\frac{\xi\sigma_e^0}{m_{\chi^0}} = 7 \times 10^{-3}$ pb/GeV. The vertical line indicates the energy threshold of the DAMA/NaI experiment.

It is possible to see that—due to the behavior of the momentum distribution of the electrons, $\rho(p)$, at high p and due to the behavior of the I function at low p [related to the $f(\vec{v}_{\chi^0})$ behavior at high velocity]—the main contribution to the counting rate in NaI(Tl) detectors with energy threshold at 2 keV comes from electrons with momenta around few MeV$/c$ [see Fig. 3(b)]. It is worthwhile to note that similar behaviors can also be obtained by using other choices of the halo model.

Finally, an example of the shapes of expected energy distributions in NaI(Tl) due to χ^0 interactions with electrons for the A5 halo model (a NFW halo model with local velocity equal to 220 km/s and density equal to the maximum value, see Refs. [14,34]) is reported in Fig. 4. In this example the normalization factor is $\frac{\xi\sigma_e^0}{m_{\chi^0}} = 7 \times 10^{-3}$ pb/GeV.

IV. DATA ANALYSIS AND RESULTS FOR ELECTRON INTERACTING DM CANDIDATE IN DAMA/NaI

The 6.3σ C.L. model independent evidence for dark matter particles in the galactic halo achieved over seven annual cycles by DAMA/NaI [14,15] (total exposure $\simeq 1.1 \times 10^5$ kg $\times$ days) can also be investigated for the case of an electron interacting DM candidate (in addition to the other corollary quests already mentioned at the end of Sec. I).

In the analysis presented here, the same dark halo models and related parameters given in Table VI of Ref. [14] have been used; the related DM density is given in Table VII of the same reference. Moreover, here $\eta_e = 2.6 \times 10^{26}$ kg^{-1} and the halo escaping velocity has been taken equal to 650 km/s.

The results are calculated by taking into account the time and energy behaviors of the *single-hit* experimental data through the standard maximum likelihood method.[3] In particular, they are presented in terms of the allowed interval of the $\frac{\xi\sigma_e^0}{m_{\chi^0}}$ parameter, obtained as superposition of the configurations corresponding to likelihood function values *distant* more than 4σ from the null hypothesis (absence of modulation) in each one of the several (but still a very limited number) of the considered model frameworks. This allows us to account for at least some of the existing theoretical and experimental uncertainties (see e.g. in Refs. [14–19] and in literature).

For these scenarios the DAMA/NaI annual modulation data gives for the considered χ^0 candidate: 1.1×10^{-3} pb/GeV $< \frac{\xi\sigma_e^0}{m_{\chi^0}} < 42.7 \times 10^{-3}$ pb/GeV at 4σ from null hypothesis. In particular, Fig. 5 shows the DAMA/NaI region allowed in the ($\xi\sigma_e^0$ vs m_{χ^0}) plane for the same dark halo models and related parameters described in Ref. [14].

We would like to stress that—although the above-mentioned calculations have been made for the $V \pm A$ and for the scalar 4-fermion contact interactions—the results given here hold for every kind of DM candidate interacting with electrons and with cross section σ_e having a weak dependence on p and v_{χ^0}, that is $\sigma_e \sim \sigma_e^0$; in such a case, the DAMA/NaI annual modulation data gives 1.6×10^{-3} pb/GeV $< \frac{\xi\sigma_e^0}{m_{\chi^0}} < 53.4 \times 10^{-3}$ pb/GeV at 4σ from null hypothesis.

Let us now comment on some phenomenological implications about the possible mediator of the interaction (hereafter U boson). The hypothesis of 4-fermion contact interaction still holds for U boson masses, M_U, larger than the transferred momentum ($M_U \gtrsim 10$ MeV). In the pure $V \pm A$ and pure scalar scenario, the cross section is given by (see Appendix B)

$$\sigma_e^0 = \frac{\overline{|M|^2}}{16\pi m_{\chi^0}^2} = \frac{16G^2 m_{\chi^0}^2 m_e^2}{16\pi m_{\chi^0}^2} = \frac{G^2 m_e^2}{\pi} = \frac{c_e^2 c_{\chi^0}^2 m_e^2}{\pi M_U^4}. \quad (13)$$

[3]Shortly, the likelihood function is $\mathbf{L} = \mathbf{\Pi}_{ijk} e^{-\mu_{ijk}} \frac{\mu_{ijk}^{N_{ijk}}}{N_{ijk}!}$, where N_{ijk} is the number of events collected in the ith time interval, by the jth detector and in the kth energy bin. N_{ijk} follows a Poissonian distribution with expectation value $\mu_{ijk} = [b_{jk} + S_{0,k} + S_{m,k} \cos\omega(t_i - t_0)] M_j \Delta t_i \Delta E \epsilon_{jk}$. The unmodulated and modulated parts of the signal, $S_{0,k}$ and $S_{m,k} \cos\omega(t_i - t_0)$, respectively, are here functions of the only free parameter of the fit: the $\frac{\xi\sigma_e^0}{m_{\chi^0}}$ ratio. The b_{jk} is the background contribution; Δt_i is the detector running time during the ith time interval; ϵ_{jk} is the overall efficiency and M_j is the detector mass.

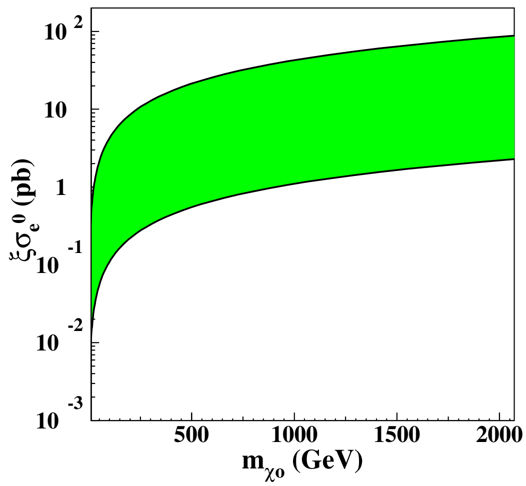

FIG. 5 (color online). The DAMA/NaI region allowed in the ($\xi\sigma_e^0$ vs m_{χ^0}) plane for the same dark halo models and related parameters described in Ref. [14]. The region encloses configurations corresponding to likelihood function values *distant* more than 4σ from the null hypothesis (absence of modulation). We note that, although the mass region in the plot is up to 2 TeV, χ^0 particles with larger masses are also allowed.

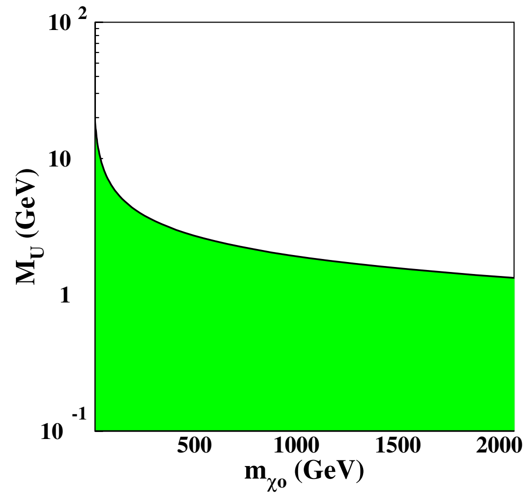

FIG. 6 (color online). Region of U boson mass allowed by present analysis and by the $g_e - 2$ constraint [4] considering that $\xi \leq 1$ and that the theory is perturbative ($c_{\chi^0} < \sqrt{4\pi}$). See text. There the U boson with M_U masses in the sub-GeV range required by the analyses of Refs. [1,4,7,8] is well allowed for a large interval of m_{χ^0}.

The effective coupling constant, G, depends on the couplings, c_e and c_{χ^0}, of the U boson with the electron and the χ^0 particle, respectively. We note that limits on c_e have been achieved by the experimental constraints on the possible U boson coupling to electron arising from the $g_e - 2$ measurements: $c_e \lesssim 10^{-4} \frac{M_U}{\mathrm{MeV}}$ [4]. Moreover, more restrictive limits have been obtained under the assumption of universality ($c_\mu \sim c_e \sim c_\nu$) by considering the $g_\mu - 2$ and $\nu - e$ scattering data: $\lesssim 3 \times 10^{-6} \frac{M_U}{\mathrm{MeV}}$ [4].

The DAMA/NaI allowed region of Fig. 5 requires values of c_e well in agreement with these experimental upper limits. In fact, from Fig. 5 and reminding that $\xi \leq 1$ and $m_{\chi^0} \gtrsim$ few GeV (see above), we obtain that $\sigma_e^0 \gtrsim 10^{-2}$ pb. Requiring that the theory remains perturbative (that is, $c_{\chi^0} < \sqrt{4\pi}$) and for $M_U \sim 10$ MeV, the values of c_e allowed by DAMA/NaI data are [see Eq. (13)] $c_e \gtrsim 5 \times 10^{-7}$, in agreement with the experimental upper limits.

More in general, considering the limit on c_e from $g_e - 2$ data and the obtained lower bound $\frac{\xi\sigma_e^0}{m_{\chi^0}} > 1.1 \times 10^{-3}$ pb/GeV from the DAMA/NaI data, the allowed U boson masses are $M_U(\mathrm{GeV}) \lesssim \sqrt{\frac{3700}{m_{\chi^0}(\mathrm{GeV})}}$, as reported in Fig. 6. There the U boson with M_U masses in the sub-GeV range required by the analyses of Refs. [1,4,7–10] is well allowed for a large interval of m_{χ^0}.

V. CONCLUSIONS

In this paper, the scenario of a DM particle χ^0 with dominant interaction with electrons has been investigated. This candidate can be directly detected only through its interaction with electrons in suitable detectors. Theoretical arguments have been developed and related phenomenological aspects have been discussed. In particular, the impact of these DM candidates has also been analyzed in a phenomenological framework on the basis of the DAMA/NaI data.

For the considered dark halo models, the DAMA/NaI data support for the χ^0 candidate: 1.1×10^{-3} pb/GeV $< \frac{\xi\sigma_e^0}{m_{\chi^0}} < 42.7 \times 10^{-3}$ pb/GeV at 4σ from null hypothesis. Allowed regions for the characteristic phenomenological parameters of the model have been presented. The obtained allowed interval for the mass of the possible mediator of the interaction is well in agreement with the typical requirements of the phenomenological analyses available in literature.

Finally, we further remind that the U boson interpretation is not the unique one since, for example, there are domains in general SUSY parameter space where the LSP-electron interaction can dominate LSP-quark one.

APPENDIX A: χ^0 INTERACTION WITH ATOMS

The inclusive scattering of a χ^0 particle on an atom A is here analyzed: $\chi^0 A \to \chi^0 X$, where X denotes the final state of the atom. The cross section of the process is obtained by summing over the possible contributions of all the X final states:

$$d\sigma_{\chi^0 A} \propto \sum_X |T_{AX}|^2 = \sum_X \langle A, \chi^0(k) | \chi^0(k'), X \rangle \langle X, \chi^0(k') | \chi^0(k), A \rangle; \quad \text{(A1)}$$

here T_{AX} is the transition amplitude when the final state is X.

Since it has been assumed that the interaction of χ^0 with the electrons is dominant, we can use a full set of electronic plane wave functions, $e(p)$, and rewrite:

$$\langle A, \chi^0(k)| = \sum_p \langle A|e(p)\rangle\langle e(p), \chi^0(k)| \tag{A2}$$

$$|\chi^0(k'), X\rangle = \sum_{p'} \langle e(p')|X\rangle|\chi^0(k'), e(p')\rangle. \tag{A3}$$

Therefore

$$T_{AX} = \sum_{p,p'} \langle A|e(p)\rangle T_{(p+k-p'-k')}\langle e(p')|X\rangle, \tag{A4}$$

where $T_{(p+k-p'-k')} = \langle e(p), \chi^0(k)|\chi^0(k'), e(p')\rangle \propto M \times \delta(p + k - p' - k')$ is the transition amplitude for free electron $-\chi^0$ elastic scattering and M is the matrix element reported in Eq. (3).

Since X is whatever final state: $\sum_X \langle e(p')|X\rangle\langle X|e(p'')\rangle = \delta(p' - p'')$; therefore, Eq. (A1) can be written as

$$\sum_X T_{AX}^2 = \sum_{p,p',p'''} \langle A|e(p)\rangle T_{(p+k-p'-k')} T^*_{(p'''+k-p'-k')}\langle e(p''')|A\rangle$$
$$\propto \sum_{p,p'} \rho(p)|M|^2\delta(p+k-p'-k'), \tag{A5}$$

where $\rho(p) = |\langle A|e(p)\rangle|^2$ is the momentum distribution function of the electrons in the atom A. Finally, we can deduce $d\sigma_{\chi^0 A} = d\sigma_{\chi^0 e}\rho(p)d^3p$, where $d\sigma_{\chi^0 e}$ is the $\chi^0 - e^-$ elastic scattering cross section given in Eq. (3).

APPENDIX B: THE INVARIANT AMPLITUDE FOR $\chi^0 - e^-$ ELASTIC SCATTERING

In the following we consider the elastic scattering of the χ^0 fermion on an electron by using a Fermi-like 4-fermion contact interaction.

1. The VA subcase

The squared matrix element, averaged over the initial spins and summed over the final ones, can be written as

$$\overline{|M_{VA}|^2} = G^2 L^{\mu\nu}_{(\chi^0)} L^{(e)}_{\mu\nu}, \tag{B1}$$

where

$$L^{\mu\nu}_{(\chi^0)} = \frac{1}{2}\sum_{\text{spin}}[\bar{U}_{\chi^0}(k')\gamma^\mu(g_V + g_A\gamma^5)U_{\chi^0}(k)]$$
$$\times [\bar{U}_{\chi^0}(k)\gamma^\nu(g_V + g_A\gamma^5)U_{\chi^0}(k')] \tag{B2}$$

$$L^{(e)}_{\mu\nu} = \frac{1}{2}\sum_{\text{spin}}[\bar{U}_e(p')\gamma_\mu(c_V + c_A\gamma^5)U_e(p)]$$
$$\times [\bar{U}_e(p)\gamma_\nu(c_V + c_A\gamma^5)U_e(p')]. \tag{B3}$$

Let us focus just on Eq. (B2), since Eq. (B3) has the same structure. One can write

$$L^{\mu\nu}_{(\chi^0)} = \tfrac{1}{2}\mathrm{Tr}[(\not{k}' + m_{\chi^0})\gamma^\mu(g_V + g_A\gamma^5)(\not{k} + m_{\chi^0}) \times \gamma^\nu(g_V + g_A\gamma^5)]$$
$$= T^{AA} + T^{VA} + T^{AV} + T^{VV}. \tag{B4}$$

The four terms can be explicated as

$$T^{AA} = \tfrac{1}{2}\mathrm{Tr}[(\not{k}' + m_{\chi^0})\gamma^\mu g_A\gamma^5(\not{k} + m_{\chi^0})\gamma^\nu g_A\gamma^5] \tag{B5}$$

$$T^{VV} = \tfrac{1}{2}\mathrm{Tr}[(\not{k}' + m_{\chi^0})\gamma^\mu g_V(\not{k} + m_{\chi^0})\gamma^\nu g_V] \tag{B6}$$

$$T^{AV} = \tfrac{1}{2}\mathrm{Tr}[(\not{k}' + m_{\chi^0})\gamma^\mu g_A\gamma^5(\not{k} + m_{\chi^0})\gamma^\nu g_V] \tag{B7}$$

$$T^{VA} = \tfrac{1}{2}\mathrm{Tr}[(\not{k}' + m_{\chi^0})\gamma^\mu g_V(\not{k} + m_{\chi^0})\gamma^\nu g_A\gamma^5] \tag{B8}$$

By using trace theorems, one gets

$$T^{AA} = \tfrac{1}{2}g_A^2\,\mathrm{Tr}[\not{k}'\gamma^\mu\not{k}\gamma^\nu - m^2_{\chi^0}\gamma^\mu\gamma^\nu]$$
$$= 2g_A^2(k'^\mu k^\nu + k'^\nu k^\mu - k'kg^{\mu\nu} - m^2_{\chi^0}g^{\mu\nu}) \tag{B9}$$

$$T^{VV} = \tfrac{1}{2}g_V^2\,\mathrm{Tr}[\not{k}'\gamma^\mu\not{k}\gamma^\nu + m^2_{\chi^0}\gamma^\mu\gamma^\nu]$$
$$= 2g_V^2(k'^\mu k^\nu + k'^\nu k^\mu - k'kg^{\mu\nu} + m^2_{\chi^0}g^{\mu\nu}) \tag{B10}$$

$$T^{AV} = \tfrac{1}{2}\mathrm{Tr}[(\not{k}' + m_{\chi^0})\gamma^\mu(\not{k} - m_{\chi^0})\gamma^\nu g_A\gamma^5 g_V] \tag{B11}$$

$$T^{VA} = \tfrac{1}{2}g_V g_A\,\mathrm{Tr}[\gamma^5\not{k}'\gamma^\mu\not{k}\gamma^\nu] = T^{AV} \tag{B12}$$

$$T^{VA} + T^{AV} = -g_V g_A 4i\varepsilon^{\alpha\mu\beta\nu}k'_\alpha k_\beta. \tag{B13}$$

Thus, one can write

$$L^{\mu\nu}_{(\chi^0)} = 2(g_V^2 + g_A^2)[k'^\mu k^\nu + k'^\nu k^\mu - k'kg^{\mu\nu}]$$
$$+ 2(g_V^2 - g_A^2)m^2_{\chi^0}g^{\mu\nu} - 4g_V g_A i\varepsilon^{\alpha\mu\beta\nu}k'_\alpha k_\beta. \tag{B14}$$

Finally, the matrix element for the process can be written as

$$\overline{|M_{VA}|^2} = 8G^2[A(p'k')(pk) + B(p'k)(pk') - C(kk')m_e^2 - D(pp')m^2_{\chi^0}], \tag{B15}$$

where

$$\begin{aligned} A &= (g_V^2 + g_A^2)(c_V^2 + c_A^2) + 4g_V g_A c_V c_A \\ &= (c_V g_V + c_A g_A)^2 + (c_V g_A + c_A g_V)^2 \\ B &= (g_V^2 + g_A^2)(c_V^2 + c_A^2) - 4g_V g_A c_V c_A \\ &= (c_V g_V - c_A g_A)^2 + (c_V g_A - c_A g_V)^2 \\ C &= (g_V^2 + g_A^2)(c_V^2 - c_A^2) \\ D &= (g_V^2 - g_A^2)(c_V^2 + c_A^2). \end{aligned} \tag{B16}$$

In the case of $V \pm A$ interaction ($|c_V| = |c_A|$ and $|g_V| = |g_A|$), the matrix element is

$$\overline{|M_{V\pm A}|^2} = 8G^2[A(p'k')(pk) + B(p'k)(pk')] \tag{B17}$$

knowing that χ^0 is not relativistic (see text), one obtains $(p'k')(pk) \simeq p_0' k_0' p_0 k_0$ and $(p'k)(pk') \simeq p_0' k_0' p_0 k_0$; moreover, for $E_d \sim$ keV one has $p_0' \simeq p_0$, giving

$$\overline{|M_{V\pm A}|^2} \simeq 16 G_{V\pm A}^2 m_{\chi^0}^2 p_0^2, \tag{B18}$$

where the Fermi effective coupling constant is $G_{V\pm A}^2 = G^2(c_V^2 + c_A^2)(g_V^2 + g_A^2)$. For this particular case, the dependence on v_{χ^0} can be neglected, while the dependence on p is included in $p_0^2 = p^2 + m_e^2$.

2. The *SP* subcase

Similarly as above, one has

$$\overline{|M_{SP}|^2} = G^2 L_{(\chi^0)} L_{(e)} \tag{B19}$$

$$L_{(\chi^0)} = \frac{1}{2}\sum_{\text{spin}} [\bar{U}_{\chi^0}(k')(g_S + i g_P \gamma^5) U_{\chi^0}(k)] \times [\bar{U}_{\chi^0}(k)(g_S + i g_P \gamma^5) U_{\chi^0}(k')] \tag{B20}$$

$$\begin{aligned} L_{(\chi^0)} &= \tfrac{1}{2}\mathrm{Tr}[(\not{k}' + m_{\chi^0})(g_S + i g_P \gamma^5)(\not{k} + m_{\chi^0}) \\ &\quad \times (g_S + i g_P \gamma^5)] \\ &= T^{SS} + T^{SP} + T^{PS} + T^{PP}. \end{aligned} \tag{B21}$$

There

$$T^{SS} = \tfrac{1}{2} g_S^2 \,\mathrm{Tr}[(\not{k}' + m_{\chi^0})(\not{k} + m_{\chi^0})] = 2 g_S^2 (k'k + m_{\chi^0}^2) \tag{B22}$$

$$\begin{aligned} T^{PP} &= -\tfrac{1}{2} g_P^2 \,\mathrm{Tr}[(\not{k}' + m_{\chi^0})\gamma^5(\not{k} + m_{\chi^0})\gamma^5] \\ &= 2 g_p^2 (k'k - m_{\chi^0}^2) \end{aligned} \tag{B23}$$

$$T^{PS} = \tfrac{1}{2} i g_P g_S \,\mathrm{Tr}[(\not{k}' + m_{\chi^0})\gamma^5(\not{k} + m_{\chi^0})] \tag{B24}$$

$$T^{SP} + T^{PS} = i g_P g_S \,\mathrm{Tr}[(\not{k}' + m_{\chi^0})\gamma^5 m_{\chi^0}] = 0 \tag{B25}$$

Hence,

$$\begin{aligned} L_{(\chi^0)} &= 2[(g_S^2 + g_P^2)k'k + (g_S^2 - g_P^2) m_{\chi^0}^2] \\ &= 2(g_+ k'k + g_- m_{\chi^0}^2), \end{aligned} \tag{B26}$$

where $g_+ = g_S^2 + g_P^2 > 0$ and $g_- = g_S^2 - g_P^2$. Finally,

$$\begin{aligned} \overline{|M_{SP}|^2} &= 4G^2[g_+ c_+ (k'k)(p'p) + g_+ c_- (k'k) m_e^2 \\ &\quad + g_- c_+ (p'p) m_{\chi^0}^2 + g_- c_- m_{\chi^0}^2 m_e^2]. \end{aligned} \tag{B27}$$

In the particular pure scalar case ($g_P = c_P = 0$), one obtains

$$\begin{aligned} \overline{|M_S|^2} &= 4G^2 g_S^2 c_S^2 [(k'k) + m_{\chi^0}^2][(p'p) + m_e^2] \\ &\simeq 8 G_S^2 m_{\chi^0}^2 [p_0' p_0 - \vec{p}' \vec{p} + m_e^2]. \end{aligned} \tag{B28}$$

Thus, considering the momentum distribution of atomic electron, for $E_d \sim$ keV practically $\vec{p}' \sim -\vec{p}$ and, therefore,

$$\overline{|M_S|^2} \sim 16 G_S^2 m_{\chi^0}^2 p_0^2, \tag{B29}$$

where the Fermi effective coupling constant is $G_S^2 = G^2 c_S^2 g_S^2$.

Also in this case there is a negligible dependence from v_{χ^0} and a weak dependence from p.

[1] Y. Ascasibar, P. Jean, C. Boehm, and J. Knoedlseder, Mon. Not. R. Astron. Soc. **368**, 1695 (2006); C. Jacoby and S. Nussinov, J. High Energy Phys. 05 (2007) 017.

[2] D. P. Finkbeiner and N. Weiner, Phys. Rev. D **76**, 083519 (2007).

[3] M. Pospelov and A. Ritz, Phys. Lett. B **651**, 208 (2007).

[4] P. Fayet, Phys. Rev. D **75**, 115017 (2007).

[5] J. Knodlseder *et al.*, Astron. Astrophys. **441**, 513 (2005); P. Jean *et al.*, Astron. Astrophys. **407**, L55 (2003); J. Knodlseder *et al.*, Astron. Astrophys. **411**, L457 (2003).

[6] C. Boehm and Y. Ascasibar, Phys. Rev. D **70**, 115013 (2004); G. Weidenspointner *et al.*, arXiv:astro-ph/0702621.

[7] B. Tatischeff and E. Tomasi-Gustafsson, arXiv:0710.1796; arXiv:0710.1798.

[8] N. G. Deshpande, G. Eilam, and J. Jiang, Phys. Lett. B **632**, 212 (2006); D. S. Gorbunov and V. A. Rubakov, Phys. Rev. D **73**, 035002 (2006); C. H. Chen *et al.*, arXiv:0708.0937.

[9] T. Walcher, arXiv:hep-ph/0111279.

[10] F. W. N. de Boer *et al.*, J. Phys. G **27**, L29 (2001); **23**, L85 (1997); Nucl. Phys. B, Proc. Suppl. **72**, 189 (1999); M. El-Nadi and O. E. Badawy, Phys. Rev. Lett. **61**, 1271 (1988); K. Asakimori *et al.*, J. Phys. G **25**, L133 (1999).

[11] R. Foot, H. Lew, and R. R. Volkas, Phys. Rev. D **44**, 859 (1991).

[12] K. S. Babu, E. Ma, and S. Willenbrock, Phys. Rev. D **69**, 051301(R) (2004); S. L. Chen and E. Ma, Mod. Phys. Lett. A **19**, 1267 (2004); A. Demaria, C. I. Low, and R. R. Volkas, Phys. Rev. D **72**, 075007 (2005).

[13] R. Foot and H. Lew, Phys. Rev. D **41**, 3502 (1990); R. Foot, H. Lew, and R. R. Volkas, Phys. Rev. D **44**, 1531 (1991); R. Foot and R. R. Volkas, Phys. Lett. B **645**, 345 (2007); K. S. Babu, T. W. Kephart, and H. Pas,

arXiv:0709.0765.
[14] R. Bernabei *et al.*, Riv. Nuovo Cimento Soc. Ital. Fis. **26**, 1 (2003).
[15] R. Bernabei *et al.*, Int. J. Mod. Phys. D **13**, 2127 (2004).
[16] R. Bernabei *et al.*, Eur. Phys. J. C **47**, 263 (2006).
[17] R. Bernabei *et al.*, Int. J. Mod. Phys. A **22**, 3155 (2007).
[18] R. Bernabei *et al.*, Int. J. Mod. Phys. A **21**, 1445 (2006).
[19] R. Bernabei *et al.*, arXiv:0710.0288 [Eur. Phys. J. C (to be published)].
[20] A. Bottino *et al.*, Phys. Rev. D **67**, 063519 (2003); **68**, 043506 (2003).
[21] A. Bottino *et al.*, Phys. Rev. D **69**, 037302 (2004).
[22] A. Bottino *et al.*, Phys. Lett. B **402**, 113 (1997); **423**, 109 (1998); Phys. Rev. D **59**, 095004 (1999); **59**, 095003 (1999); Astropart. Phys. **10**, 203 (1999); **13**, 215 (2000); Phys. Rev. D **62**, 056006 (2000); **63**, 125003 (2001); Nucl. Phys. **B608** 461 (2001).
[23] K. Belotsky, D. Fargion, M. Khlopov, and R. V. Konoplich, arXiv:hep-ph/0411093.
[24] D. Smith and N. Weiner, Phys. Rev. D **64**, 043502 (2001); D. Tucker-Smith and N. Weiner, Phys. Rev. D **72**, 063509 (2005).
[25] R. Foot, Phys. Rev. D **69**, 036001 (2004).
[26] S. Mitra, Phys. Rev. D **71**, 121302(R) (2005).
[27] E. M. Drobyshevski *et al.*, arXiv:0704.0982.
[28] E. M. Drobyshevski, arXiv:0706.3095.
[29] C. Arina and N. Fornengo, arXiv:0709.4477.
[30] A. Bottino *et al.*, arXiv:0710.0553.
[31] F. Biggs *et al.*, At. Data Nucl. Data Tables **16**, 201 (1975).
[32] D. Brusa *et al.*, Nucl. Instrum. Methods Phys. Res., Sect. A **379**, 167 (1996).
[33] R. Ribberfors *et al.*, Phys. Rev. A **26**, 3325 (1982); Phys. Rev. B **12**, 2067 (1975).
[34] P. Belli *et al.*, Phys. Rev. D **66**, 043503 (2002).